Research Article | Vol. 27, No. 24 / 25 November 2019 / Optics Express 34552
Optics EXPRESS

2166 nm all-fiber short-pulsed Raman laser based on germania-core fiber

TUANJIE DU,[1,2,5] YANHONG LI,[2,5] HONGJIAN WANG,[2] ZHIHAO CHEN,[1,4] VALERY M. MASHINSKY,[3] AND ZHENGQIAN LUO[2,*]

[1]Research center for photonics technology, Quanzhou Normal University, Quanzhou 362000, China
[2]Department of Electronic Engineering, Xiamen University, Xiamen 361005, China
[3]Fiber Optics Research Center, Russian Academy of Sciences, Moscow 119333, Russia
[4]zhihaochen@qztc.edu.cn
[5]These authors contributed equally to this work
[*]zqluo@xmu.edu.cn

Abstract: We report a compact 2166 nm germania-fiber short-pulsed Raman laser based on the cavity matching scheme. The all-fiber Raman cavity is formed by a pair of 2166 nm fiber Bragg gratings. High-power noise-like pulses from a 1981 nm fiber laser are used to pump a 22 m germania-core fiber for providing Raman gain at ~2166 nm, and readily realizes the Raman-cavity synchronization with high mismatching tolerance. Stable Raman pulses at 2166 nm are therefore generated with the tunable pulse width of 0.9-4.4 ns and the large pulse energy up to 12.15 nJ. This is, to the best of our knowledge, the first demonstration of all-fiber short-pulsed Raman laser in the mid-infrared region.

1. Introduction

Mid-infrared (MIR, 2-20 μm) [1] short-pulsed laser sources have attracted considerable attention due to their potential applications, such as medical surgery, chemical sensing, material processing, nonlinear frequency conversion, eye-safe LIDAR and missile countermeasures [1–7]. Compared with solid-state lasers [8,9], the fast-developed fiber lasers in the MIR region have been focused owing to their advanced remarkable merits (e.g. compactness, low cost, ease of use, and maintenance-free operation). Nowadays, MIR fiber laser sources have been widely investigated using rare-earth-doped (Er^{3+}, Ho^{3+}, Dy^{3+}) ZBLAN fibers [10–20]. 12 W actively Q-switched Er:ZBLAN fiber laser at 2.8 μm with a pulse energy of 100 μJ and pulse duration of 90 ns has been reported [10]. Passively Q-switched fiber laser using nanomaterials as the saturable absorber has been achieved around 3 μm [11–13]. Wavelength-tunable gain-switched MIR fiber lasers around 3 μm have also been presented [14]. Furthermore, mode-locked MIR rare-earth-doped fiber lasers for ultrashort pulse generation have made considerable progress in recent years. Sub-picosecond pulse generation in 2.8 μm Er:ZBLAN fibers have been successfully achieved with a nonlinear polarization rotation technique [15,16] or a black phosphorus saturable absorber [17], and the mode-locked wavelength has been further extended to 3.5 μm [18]. Most recently, the most widely tunable picosecond pulses generation from 2.97 to 3.30 μm has been reported in a dysprosium-doped fluoride fiber laser with a pulse energy of 2.7 nJ [19]. However, so far MIR ultrafast rare-earth-doped fiber lasers are still restricted to the wavelengths of 2.8-3.3 μm and 3.5 μm [21]; and it is well known that silica-based ultrafast fiber lasers are generally limited to <2.1 μm [22–26]. It is noteworthy that ultrafast fiber laser in the spectrum gap between 2.1 to 2.7 μm has not been fully exploited yet. Raman gain in optical fiber is available to overcome the spectral limitation, since the simulated Raman scattering can be excited virtually at any wavelength by providing a suitable pump source. Therefore, ultrafast Raman fiber laser with the advantage of wavelength flexibility may offer an opportunity and powerful weapon to attack the spectral gap (2.1 to 2.7 μm).

#374165 https://doi.org/10.1364/OE.27.034552
Journal © 2019 Received 31 Jul 2019; revised 29 Sep 2019; accepted 28 Oct 2019; published 11 Nov 2019

Optics EXPRESS

Due to the silica-fiber loss arising rapidly in >2 μm wavelength range and low Raman gain, soft-glass specialty fibers (e.g. fluoride glass and chalcogenide glass) with the MIR transparency and high Raman coefficient have been recognized as strong candidates for MIR Raman lasers [27–31]. 3.7 W fluoride glass Raman fiber laser operating at 2231 nm has been demonstrated with a laser slope efficiency of 15%[27]. Most recently, Raman fiber laser emitting in the MIR at 3.34 μm [28] and cascaded Raman fiber laser at 3.766 μm [29] has been obtained in a chalcogenide glass fiber. However, all of them still exist two restrictions: 1) requiring the bulk optical components and precluding compact MIR all-fiber integration; 2) operating at continuum wave state and impossibility of MIR short-pulsed Raman fiber laser regime. To solve these problems, germania-core fibers can offer a good opportunity to develop compact all-fiber MIR short pulse Raman laser, due to the advantages of MIR transparency in the 2-3 μm wavelength range, fusion splicing to standard silica fibers, large nonlinear coefficient and the ease ofNL manufacture.

In this paper, we experimentally demonstrated a 2166 nm all-fiber short-pulsed Raman fiber laser based on germania-core fiber and the cavity matching scheme. The MIR Raman laser consists of two highly reflective fiber Bragg gratings (HR FBGs) and 22 m germania-core Raman fiber pumped by a 1981 nm homemade noise-like pulse (NLP) mode-locked fiber laser. Benefiting from the cavity matching scheme, the MIR Raman cavity is well synchronized to the 1981 nm mode-locked fiber laser cavity. The 2166 nm Raman laser produced the maximum output power of 52.65 mW, pulse energy of 12.15 nJ and minimum pulse duration of 900 ps.

2. Experimental set-up and operation principle

The experimental setup of the 2166 nm all-fiber germania-core Raman laser system is shown in Fig. 1(a). A 1981 nm NLP mode-locked Tm-doped fiber laser (TDFL) is firstly built as the pump laser. The FLM is not only used as an output mirror, but also acts as a periodic saturable absorber for initiating high power NLP mode-locked laser. A 10/90 OC is placed at the output of 1981 nm mode locked laser for monitoring the 1981 nm NLP mode-locking operation. In the experiment, the 2166 nm Raman fiber laser consists of two HR FBGs and 22 m germania-core Raman fiber which has the same parameters as presented in [32] with germania-core concentration of 97%,

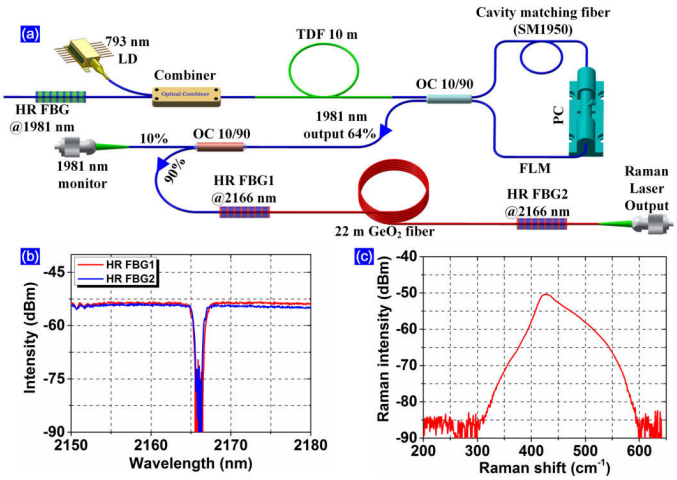

Fig. 1. (a) Experiment setup of the 2166 nm all-fiber germania-core Raman laser system. LD: laser diode, HR FBG: high reflectivity fiber Bragg grating, TDF: thulium-doped fiber, OC: optical coupler, PC: polarization controller, FLM: fiber loop mirror. (b) The transmission spectra of the two HR FBGs at 2166 nm. (c) The Raman spectrum of the GeO_2 fiber.

Optics EXPRESS

core diameter of ~2 μm. The 1981 nm NLP laser is launched to the germania-core fiber through an input HR FBG1 to provide the Raman gain. As seen in Fig. 1(b), the transmission spectrum of the two FBGs are exact matched ensuring the Raman laser occurring. The Raman spectrum of the germania-core fiber is measured as given in Fig. 1(c). A broadband Raman shift is observed from 300 to 600 cm^{-1} with the Raman peak of 427 cm^{-1}, and the Raman-scattering cross section of the germania-core fiber is 5-9 times higher than one of silica glass fiber [32]. The Raman cavity round-trip frequency was synchronized [33,34] with the pump pulse repetition rate by adjusting the cavity matching fiber (SM1950) in the pump cavity. Thanks to the unique properties of the NLP pump laser with a sub-nanosecond pulse width and high peak power, the Raman Stokes wave and the pump pulses can be matched easily. A 12.5 GHz photodetector (ET-5000F, Electro-Optics Technology Inc.) together with a RF spectrum analyzer and a 40 GS/s high speed oscilloscope (Agilent DSO81204A) is used to measure the pulse characteristics.

3. Experimental results and discussion

In our experiment, the continuous-wave lasing threshold of the TDFL is 2.04 W, and self-started mode locking in the NLP state is observed when the pump power exceeded 3.24 W. Figure 2 summarizes the mode-locking characteristics at a pump power of 5.48 W. As shown in Fig. 2(a), the NLP lasing at 1981.4 nm has a linewidth of 4.11 nm. Figure 2(b) shows the typical mode-locked pulse train, which has a pulse-to-pulse interval of 230.7 ns, in accordance with the cavity round-trip time. As shown in Fig. 2(c), when the pump power is gradually increased from 3.24 to 8.24 W, the pulse became increasingly wider, and the pulse profile changed from bell-shaped to rectangular. As recorded in Fig. 2(d), the output RF spectrum of the mode-locked pulses have a fundamental repetition rate of 4.334 MHz matching the cavity length well. The RF signal-to-noise ratio is about 60.14 dB. The insets in Fig. 2(d) plotted the wideband RF spectra up to 50 and 500 MHz, respectively. Interestingly, there is a modulation frequency period of ~330 MHz in the widespan RF spectrum, which corresponds to a ~2.9 ns pulse duration as can be estimated through its Fourier transformation. In Fig. 3(a) and 3(b), the average power and pulse width are measured, and the corresponding pulse energy and peak power are calculated as a function of the pump power. As the pump power increasing, the average power, pulse energy and

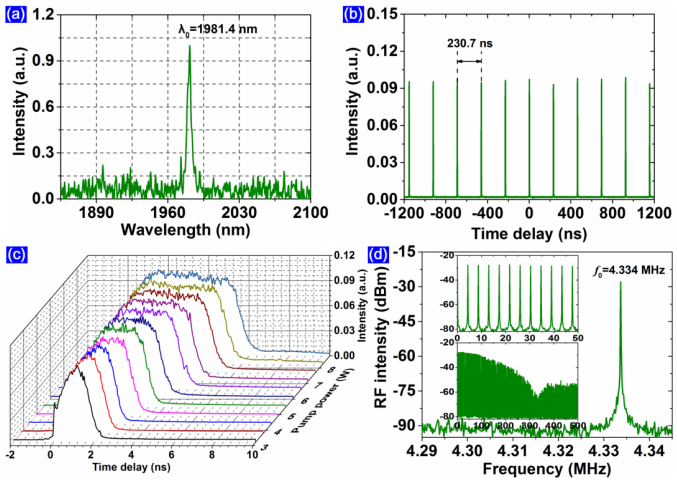

Fig. 2. The characteristics of the 1981 nm NLP mode-locking laser at a pump power of 5.48 W. (a) Optical spectrum of the NLP operation. (b) Typical oscilloscope trace. (c) Evolution of the NLP. (d) RF output spectrum at the fundamental frequency. Inset: wideband RF spectra up to 50 and 500 MHz, respectively.

Optics EXPRESS

pulse width grow linearly without the appearance of saturation. The maximum average power and highest pulse energy obtained are 2.037 W and 470 nJ, respectively. The pulse width can be tuned from 1.10 to 4.94 ns, and the peak power remained at a constant value of 95 W.

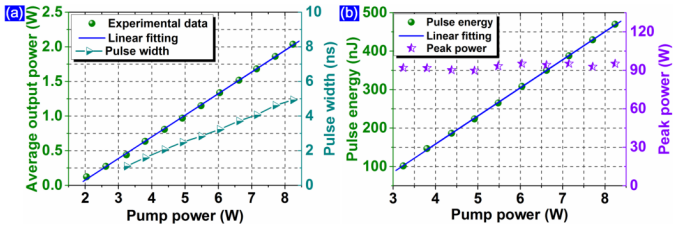

Fig. 3. (a) Average output power and pulse duration, and (b) Pulse energy and peak power as a function of the 793 nm pump power.

In order to attain the Raman laser generation, the NLP mode-locked pulses are subsequently injected into the Raman cavity. When the average injection power of the 1981 nm NLP increased over 0.376 W, we obviously observe 2166 nm laser output optical spectrum. Figure 4 summarizes the typical characteristics of the 2166 nm at the 1981 nm pump power of 0.996 W. The typical optical spectrum of the Raman laser is presented in Fig. 4(a), and the laser center wavelength locates at 2166.1 nm. The linewidth of the Raman laser is significantly broadened due to the four-wave-mixing between numerous longitudinal modes associated with long fiber laser cavity [35,36]. The significant central dip in the laser leak spectrum (after HR FBG2) is due to the reflection of the HR FBG2. As seen in the inset of Fig. 4(a), the 2166 nm Raman laser disappeares, while adjusting the PC to destroy the 1981 nm mode-locking operation. As seen in Fig. 4(b), the Raman laser has uniform pulse trains without amplitude modulation indicating a stable mode-locking operation. The pulse-to-pulse interval is measured to be 230.7 ns, which is in accordance with the 1981 nm pump laser. As shown in Fig. 4(c), when the pump power is gradually increased from 0.376 to 1.792 W, the pulse becomes increasingly wider. Figure 4(d)

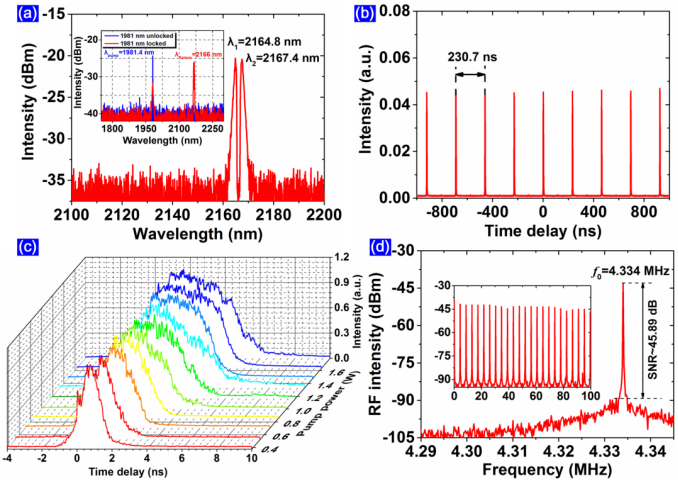

Fig. 4. Characteristics of the 2166 nm Raman fiber laser under 1981 nm pump power of 0.996 W. (a) Optical spectrum of the 2166 nm Raman laser. Inset: both the optical spectra of mode-locking and unlocked. (b) The typical oscilloscope trace. (c) Evolution of the Raman laser as the pump power of 1981 nm increased. (d) RF output spectrum at the fundamental frequency. Inset: wideband RF spectra up to 100 MHz.

Optics EXPRESS

gives the RF output spectrum of the Raman laser. The fundamental frequency peak is located at 4.334 MHz which is the same as the repetition rate of 1981 nm pumping. As seen in the inset of Fig. 4(d), the spectral peaks for ~100-MHz RF harmonics exhibit almost uniform intensity without spectral modulation, indicating good stability of our Raman pulsed laser.

For further investigating the output characteristics of our Raman laser, we record the average output power, pulse width, 1981 nm residual power as functions of the injection 1981 nm pump power. As seen in Fig. 5(a), the average output power grows linearly without appearance of saturation while the pump power increases. The pulse width increases continuously from 0.9 to 4.4 ns, and the maximum average output power is 52.65 mW, limited by the pump power. As the pump power increased, the residual 1981 nm power increases at first, and then significantly reduces due to the oscillation of the Raman laser. For further increasing the pump power, the 1981 nm residual power linearly increases. The corresponding pulse energy and peak power are calculated, as shown in Fig. 5(b). The pulse energy increases linearly from 0.95 to 12.15 nJ, and the peak power increases from 1.06 to 2.76 W.

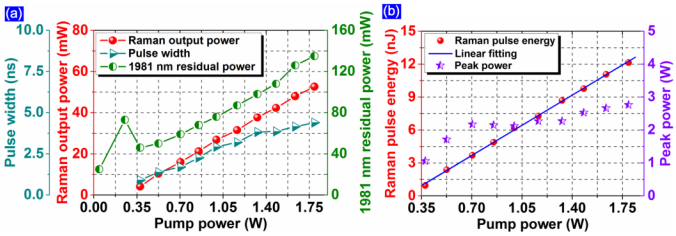

Fig. 5. (a) Average output power, pulse duration and 1981 nm residual power, and (b) Raman pulse energy and peak power as a function of the 1981 nm pump power.

4. Conclusion

In this paper, we have demonstrated an all-fiber germania-core Raman laser lasing at 2166 nm based on the cavity matching technique with high mismatching tolerance. The simply linear MIR Raman laser consists of two HR FBGs and 22 m germania-core fiber. By pumping the germania-core fiber with 1981 nm NLP mode-locked TDFL and meeting cavity matching condition, stable Raman laser operation is obtained with the maximum average output power of 52.65 mW, the maximum pulse energy of 12.15 nJ, and the minimum pulse width of 900 ps. This could provide a promising way for obtaining short Raman pulses in a compact and low-cost fiber laser.

Funding

National Natural Science Foundation of China (11674269, 61475129, 61575164); Fundamental Research Funds for the Central Universities (20720180057); Natural Science Foundation of Fujian Province for Distinguished Young Scientists (2017J06016); The Program for the Young Top Notch Talents of Fujian Province; The Program for the Nanqiang Young Top Notch Talents of Xiamen University; Tongjiang Scholar Distinguished Professor; "Harbour Project" of Quanzhou (2017ZT013).

References

1. A. Schliesser, N. Picqué, and T. W. Hänsch, "Mid-infrared frequency combs," Nat. Photonics **6**(7), 440–449 (2012).
2. F. K. Tittel, D. Richter, and A. Fried, "Mid-infrared laser applications in spectroscopy," *Top. Appl. Phys.* 89, 458–529 I. T. Sorokina and K. L. Vodopyanov, eds. (Springer-Verlag, 2003).
3. H. H. P. T. Bekman, J. C. V. D. Heuvel, F. J. M. V. Putten, and R. Schleijpen, "Development of a mid-infrared laser for study of infrared countermeasures techniques," Proc. SPIE **5615**, 27–38 (2004).

Optics EXPRESS

4. C. W. Rudy, A. Marandi, K. L. Vodopyanov, and R. L. Byer, "Octave-spanning supercontinuum generation in in situ tapered As_2S_3 fiber pumped by a thulium-doped fiber laser," Opt. Lett. **38**(15), 2865–2868 (2013).
5. K. Liu, J. Liu, H. Shi, F. Tan, and P. Wang, "High power mid-infrared supercontinuum generation in a single-mode ZBLAN fiber with up to 21.8 W average output power," Opt. Express **22**(20), 24384–24391 (2014).
6. G. Genty, J. M. Dudley, and B. J. Eggleton, "Modulation control and spectral shaping of optical fiber supercontinuum generation in the picosecond regime," Appl. Phys. B: Lasers Opt. **94**(2), 187–194 (2009).
7. T. Du, Y. Li, K. Wang, Z. Cai, H. Xu, B. Xu, V. M. Mashinsky, and Z. Luo, "2.01-2.42 μm all-fiber femtosecond Raman soliton generation in a heavily germanium doped fiber," IEEE J. Sel. Top. Quantum Electron. **25**(4), 1–7 (2019).
8. S. Vasilyev, I. Moskalev, M. Mirov, S. Mirov, and V. Gapontsev, "Multi-Watt mid-IR femtosecond polycrystalline Cr^{2+}:ZnS and Cr^{2+}:ZnSe laser amplifiers with the spectrum spanning 2.0-2.6 μm," Opt. Express **24**(2), 1616–1623 (2016).
9. N. Leindecker, A. Marandi, R. L. Byer, and K. L. Vodopyanov, "Broadband degenerate OPO for mid-infrared frequency comb generation," Opt. Express **19**(7), 6296–6302 (2011).
10. S. Tokita, M. Murakami, S. Shimizu, M. Hashida, and S. Sakabe, "12 W Q-switched Er:ZBLAN fiber laser at 2.8 μm," Opt. Lett. **36**(15), 2812–2814 (2011).
11. H. Luo, J. Li, Y. Gao, Y. Xu, X. Li, and Y. Liu, "Tunable passively Q-switched Dy^{3+}-doped fiber laser from 2.71 to 3.08 μm using PbS nanoparticles," Opt. Lett. **44**(9), 2322–2325 (2019).
12. C. Wei, X. Zhu, F. Wang, Y. Xu, K. Balakrishnan, F. Song, R. A. Norwood, and N. Peyghambarian, "Graphene Q-switched 2.78 μm Er^{3+}-doped fluoride fiber laser," Opt. Lett. **38**(17), 3233–3236 (2013).
13. Z. Qin, G. Xie, H. Zhang, C. Zhao, P. Yuan, S. Wen, and L. Qian, "Black phosphorus as saturable absorber for the Q-switched Er:ZBLAN fiber laser at 2.8 μm," Opt. Express **23**(19), 24713–24718 (2015).
14. H. Luo, J. Li, Y. Hai, X. Lai, and Y. Liu, "State-switchable and wavelength-tunable gain-switched mid-infrared fiber laser in the wavelength region around 2.94 μm," Opt. Express **26**(1), 63–79 (2018).
15. S. Duval, M. Bernier, V. Fortin, J. Genest, M. Piché, and R. Vallée, "Femtosecond fiber lasers reach the mid-infrared," Optica **2**(7), 623–626 (2015).
16. T. Hu, S. D. Jackson, and D. D. Hudson, "Ultrafast pulses from a mid-infrared fiber laser," Opt. Lett. **40**(18), 4226–4228 (2015).
17. Z. Qin, G. Xie, C. Zhao, S. Wen, P. Yuan, and L. Qian, "Mid-infrared mode-locked pulse generation with multilayer black phosphorus as saturable absorber," Opt. Lett. **41**(1), 56–59 (2016).
18. Z. Qin, T. Hai, G. Xie, J. Ma, P. Yuan, L. Qian, L. Li, L. Zhao, and D. Shen, "Black phosphorus Q-switched and mode-locked mid-infrared Er:ZBLAN fiber laser at 3.5 μm wavelength," Opt. Express **26**(7), 8224–8231 (2018).
19. R. I. Woodward, M. R. Majewski, and S. D. Jackson, "Mode-locked dysprosium fiber laser: Picosecond pulse generation from 2.97 to 3.30 μm," APL Photonics **3**(11), 116106 (2018).
20. J. Li, T. Hu, and S. D. Jackson, "Dual wavelength Q-switched cascade laser," Opt. Lett. **37**(12), 2208–2210 (2012).
21. S. D. Jackson, "Towards high-power mid-infrared emission from a fibre laser," Nat. Photonics **6**(7), 423–431 (2012).
22. T. Du, Z. Luo, R. Yang, Y. Huang, Q. Ruan, Z. Cai, and H. Xu, "1.2-W average-power, 700-W peak-power, 100-ps dissipative soliton resonance in a compact Er:Yb co-doped double-clad fiber laser," Opt. Lett. **42**(3), 462–465 (2017).
23. X. He, A. Luo, W. Lin, Q. Yang, T. Yang, X. Yuan, S. Xu, W. Xu, Z. Luo, and Z. Yang, "A stable 2 μm passively Q-switched fiber laser based on nonlinear polarization evolution," Laser Phys. **24**(8), 085102 (2014).
24. J. Wang, H. Chen, Z. Jiang, J. Yin, J. Wang, M. Zhang, T. He, J. Li, P. Yan, and S. Ruan, "Mode-locked thulium-doped fiber laser with chemical vapor deposited molybdenum ditelluride," Opt. Lett. **43**(9), 1998–2001 (2018).
25. J. Wang, Z. Jiang, H. Chen, J. Li, J. Yin, J. Wang, T. He, P. Yan, and S. Ruan, "Magnetron-sputtering deposited WTe_2 for an ultrafast thulium-doped fiber laser," Opt. Lett. **42**(23), 5010–5014 (2017).
26. J. Wang, Z. Jiang, H. Chen, J. Li, J. Yin, J. Wang, T. He, P. Yan, and S. Ruan, "High energy soliton pulse generation by a magnetron-sputtering-deposition-grown $MoTe_2$ saturable absorber," Photonics Res. **6**(6), 535–541 (2018).
27. V. Fortin, M. Bernier, D. Faucher, J. Carrier, and R. Vallée, "3.7 W fluoride glass Raman fiber laser operating at 2231 nm," Opt. Express **20**(17), 19412–19419 (2012).
28. M. Bernier, V. Fortin, N. Caron, M. El-Amraoui, Y. Messaddeq, and R. Vallée, "Mid-infrared chalcogenide glass Raman fiber laser," Opt. Lett. **38**(2), 127–129 (2013).
29. M. Bernier, V. Fortin, M. El-Amraoui, Y. Messaddeq, and R. Vallée, "3.77 μm fiber laser based on cascaded Raman gain in a chalcogenide glass fiber," Opt. Lett. **39**(7), 2052–2055 (2014).
30. S. D. Jackson and G. Anzueto-Sánchez, "Chalcogenide glass Raman fiber laser," Appl. Phys. Lett. **88**(22), 221106 (2006).
31. V. Fortin, M. Bernier, J. Carrier, and R. Vallée, "Fluoride glass Raman fiber laser at 2185 nm," Opt. Lett. **36**(21), 4152–4154 (2011).
32. E. M. Dianov and V. M. Mashinsky, "Germania-based core optical fibers," J. Lightwave Technol. **23**(11), 3500–3508 (2005).
33. R. H. Stolen, C. Lin, and R. K. Jain, "A time-dispersion-tuned fiber Raman oscillator," Appl. Phys. Lett. **30**(7), 340–342 (1977).
34. R. H. Stolen, C. Lin, J. Shah, and R. F. Leheny, "A fiber Raman ring laser," IEEE J. Quantum Electron. **14**(11), 860–862 (1978).
35. J. C. Bouteiller, "Spectral modeling of Raman fiber lasers," IEEE Photonics Technol. Lett. **15**(12), 1698–1700 (2003).

Optics EXPRESS

36. S. A. Babin, D. V. Churkin, A. E. Ismagulov, S. I. Kablukov, and E. V. Podivilov, "Turbulence-induced square-root broadening of the Raman fiber laser output spectrum," Opt. Lett. **33**(6), 633–635 (2008).